

Part III: Nonlinear Behavior

Chapter 7

Perturbation Models for Stability, Phase Noise, and Modulation

The complex dynamics of coupled-oscillator arrays lead to the existence of a multitude of steady-state solutions. In addition to finding or selecting a desired steady-state solution, one further needs to guarantee its stability. In this section, perturbation methods are described that allow the designer to examine both the existence as well as the local stability of the various steady-state solutions of coupled oscillator arrays. An introduction to stability analysis of nonlinear dynamical systems is presented [94], followed by its application to coupled oscillator systems [95] [96].

The perturbation nature of noise, leads to phase-noise analysis methods that are closely related to the formulation used in the stability analysis. Analytical models are presented that demonstrate the attractive properties of coupled inter-injection locked oscillator systems, among them improved phase-noise performance compared to single elements [97].

A straightforward application of coupled-oscillator arrays has been in power-combining arrays where, by controlling the phase shift within an array of synchronized oscillator elements, one can direct the radiated beam towards a desired direction taking advantage of free-space power combining and eliminating the use of lossy power-combining networks. The simple topologies associated with such arrays have led to their consideration in communication

system applications where one introduces modulation into the oscillator signals [98,99]. Thus, methods to introduce modulation in such arrays are presented. These architectures are distinguished from mixer-oscillator arrays where the modulation is not applied in the oscillator signal. Finally, an introduction to the analysis of coupled phase-locked loops is provided.

7.1 Preliminaries of Dynamical Systems

We have demonstrated in Part I of this book that coupled-oscillator arrays are able to synchronize in frequency while maintaining a fixed distribution of the relative phases between their elements, and that, despite the complex nature of their dynamics, there are simple methods to control the phase relationships among the array elements, which require a small number of control parameters. It was also demonstrated that as the number of elements increases, there exist many different synchronized solutions, with different ensemble frequency values and different phase distributions. In order to be able to study the behavior of the various solutions as selected parameters of the array are varied, we must first provide a theoretical framework from nonlinear dynamical system theory. This will allow us to classify the types of the solutions and the phenomena that lead to creation or elimination of solutions as well as to changes in the solution stability.

In this section, principles of stability analysis of nonlinear dynamical systems are presented. The theory can be found in standard literature on dynamical systems [100] [101] and nonlinear differential equations [94].

Following Parker and Chua [101] an autonomous continuous time dynamical system is described by the system of differential equations

$$\dot{\mathbf{x}} = \mathbf{f}(\mathbf{x}) \quad (7.1-1)$$

where the N -dimensional vector $\mathbf{x} \in \mathbb{R}^N$ contains the state variables of the system, and $\mathbf{f}(\mathbf{x}): \mathbb{R}^N \rightarrow \mathbb{R}^N$ is the vector field describing the dynamics of the system. The order of system Eq. (7.1-1) is N . An initial condition $\mathbf{x}(\mathbf{t}_o) = \mathbf{x}_o$ is assumed, where typically $t_o = 0$ is set, since the vector field does not depend explicitly on time.

In contrast, a non-autonomous continuous time dynamical system is described by a system of equations of the form

$$\dot{\mathbf{x}} = \mathbf{f}(\mathbf{x}, \mathbf{t}) \quad (7.1-2)$$

where the vector field depends explicitly on time. A non-autonomous system with period T can be expressed in the format of Eq. (7.1-1) by extending the state vector by one more dimension θ defined by $\dot{\theta} = 2\pi/T$, with

$\theta(t_o) = 2\pi t_o/T$. In the following a dynamical system defined by Eq. (7.1-1) will be considered. A solution of Eq. (7.1-1) for a given initial condition is called a trajectory or orbit.

A free-running oscillator and a coupled-oscillator array are autonomous dynamical systems. They become non-autonomous when an external injection source is present.

A steady state is the asymptotic behavior of a dynamical system governed by (7.1-1) when $t \rightarrow \infty$, when the transient behavior has decayed to zero. A steady state is also called a limit set. The mathematical definition of a limit set includes the asymptotic behavior of a dynamical system both as time progresses forward ($t \rightarrow +\infty$) and backward ($t \rightarrow -\infty$), distinguishing between ω -limit sets and α -limit sets, respectively.

Steady states can be classified into four different types, equilibrium points, periodic solutions, quasi-periodic solutions, and chaotic solutions.

Equilibrium points x_o correspond to the solution of

$$f(x_o) = 0 \tag{7.1-3}$$

An equilibrium point is the DC solution of an oscillator circuit.

A periodic solution $x_o(t)$, is a solution of Eq. (7.1-1) that has a minimum period T , such as

$$x_o(t + T) = x_o(t) \tag{7.1-4}$$

for every t . A periodic solution of an autonomous system is also called a limit cycle.

A quasi-periodic solution is a solution that is equal to a countable sum of periodic solutions with non-commensurate periods, in other words:

$$x_o(t) = \sum_{i=1}^M h_i(t) \tag{7.1-5}$$

where $h_i(t)$ are periodic solutions with minimum period T_i . The various frequencies $f_i = 1/T_i$ form a linearly independent set of dimension p with $1 < p \leq M$.

Finally, any bounded steady-state behavior that cannot be classified in one of the previous types is a chaotic steady state.

An N -dimensional dynamical system can be efficiently analyzed using a Poincare map [101] [102]. The Poincare map is a transform that maps an N -dimensional continuous system to an $(N - 1)$ dimensional discrete time system. This is illustrated in Fig. 7-1. Let us consider a continuous time autonomous dynamical system described by Eq. (7.1-1), which has a periodic solution denoted by L . At some point \mathbf{x}_o of the periodic orbit, we define locally a cross-section Σ that is a surface of dimension $N - 1$ intersecting L at a non-zero angle. The periodic orbit returns to the point \mathbf{x}_o on the cross-section Σ every T second. The sequence of points on the cross-section defines a discrete time system, which is equivalent to the original continuous time system. Furthermore, the limit cycle of an N -dimensional dynamical system is represented by a point on an $N - 1$ dimensional surface. The reader is referred to the literature for a precise mathematical definition of a Poincare map for both cases of an autonomous and a non-autonomous system [101] [102]. It should be noted that the computation of a Poincare map for autonomous systems is complicated by the fact that the period of the limit cycle is not known a-priori; whereas in the case of non-autonomous systems, the sampling period T is known in advance due to the explicit dependence of Eq. (7.1-2) in time.

Having provided the fundamental definitions related to dynamical systems, and the various types of existing solutions, the stability analysis of these solutions is presented in the next section.

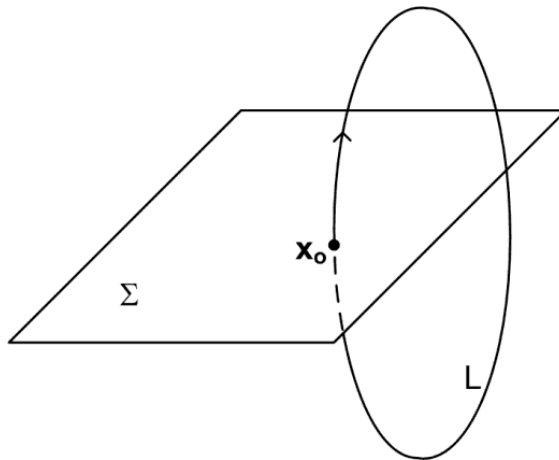


Fig. 7-1. Poincare map of a periodic orbit.

7.1.1 Introduction to Stability Analysis of Nonlinear Dynamical Systems

There exist different types of stability. For the precise mathematical definitions and types of stability, the reader is referred to the literature [94] [101]. For the purposes of this work, a rather qualitative definition is provided. A steady state \mathbf{x}_o is (Lyapunov) stable if and only if there exists a neighborhood V of \mathbf{x}_o such that every trajectory with initial condition $\mathbf{x} \in V$ remains within V at all times $t > 0$. Furthermore, a steady state is asymptotically stable if and only if there exists a neighborhood V of \mathbf{x}_o such that every trajectory with initial condition $\mathbf{x} \in V$ reaches arbitrarily close to \mathbf{x}_o given enough time $t > 0$. In other words, the ω -limit set of any initial condition within V is \mathbf{x}_o . Conversely, a steady state \mathbf{x}_o is unstable if there exists a neighborhood V of \mathbf{x}_o such that \mathbf{x}_o is the α -limit set of all initial conditions in V . Finally, a steady state \mathbf{x}_o is called non-stable if for every neighborhood V , there exists at least one point whose ω -limit set is \mathbf{x}_o and one point whose α -limit set is \mathbf{x}_o .

7.1.2 Equilibrium Point

The stability of an equilibrium point \mathbf{x}_o is examined by considering the linear perturbation of the vector field $\mathbf{f}(\mathbf{x})$ at \mathbf{x}_o . The eigenvalues of the Jacobian $\mathbf{J}(\mathbf{x}_o)$ of the vector field determine the stability of the solution.

$$\delta\dot{\mathbf{x}} = \frac{d\mathbf{f}}{d\mathbf{x}_o} \delta\mathbf{x} = \mathbf{J}(\mathbf{x}_o) \delta\mathbf{x} \tag{7.1-6}$$

with $\delta\mathbf{x}(0) = \delta\mathbf{x}_0$ representing an initial perturbation from \mathbf{x}_o . The solution of the linear differential equation Eq. (7.1-6) generally takes the form

$$\delta\mathbf{x}(t) = \sum_{i=1}^N c_i e^{\lambda_i t} \mathbf{a}_i \tag{7.1-7}$$

where λ_i and \mathbf{a}_i are the eigenvalues and eigenvectors of $\mathbf{J}(\mathbf{x}_o)$, respectively. The constants c_i are determined by the initial condition $\delta\mathbf{x}_0$.

For a given N -dimensional vector field $\mathbf{f}(\mathbf{x})$ the $N \times N$ Jacobian matrix \mathbf{J} has N eigenvalues. An equilibrium point whose eigenvalues do not have a real part equal to zero is called hyperbolic. If all eigenvalues have negative real parts, the point \mathbf{x}_o is asymptotically stable. Correspondingly, if there exists one eigenvalue with a positive real part, \mathbf{x}_o is unstable. Finally, if there exists one eigenvalue with a real part equal to zero, the equilibrium point is non-hyperbolic, a condition that is equivalent to the determinant of \mathbf{J} being equal to zero, and the eigenvalues of \mathbf{J} are not sufficient to determine its stability.

In the case of an $N = 2$ -dimensional system, the Jacobian matrix has two eigenvalues λ , which satisfy the following characteristic equation [102]

$$\lambda^2 - \sigma\lambda + \Delta = 0 \tag{7.1-8}$$

where σ is the sum and Δ the product of the two eigenvalues. The classification of the hyperbolic equilibrium points and their stability for different values of λ is shown in Fig. 7-2 [102].

7.1.3 Periodic Steady State

In order to determine the stability of a periodic solution $\mathbf{x}_o(t)$ the linear perturbation of Eq. (7.1-1), also called a linear variational equation, with respect to the time varying $\mathbf{x}_o(t)$ is formed, leading to a system of linear differential equations with periodic coefficients.

$$\delta\dot{\mathbf{x}} = \frac{d\mathbf{f}(t)}{d\mathbf{x}_o} \delta\mathbf{x} = \mathbf{J}[\mathbf{x}_o(t)]\delta\mathbf{x} \tag{7.1-9}$$

with $\delta\mathbf{x}(0) = \delta\mathbf{x}_0$ and for $\mathbf{J}[\mathbf{x}_o(t + T)] = \mathbf{J}[\mathbf{x}_o(t)]$.

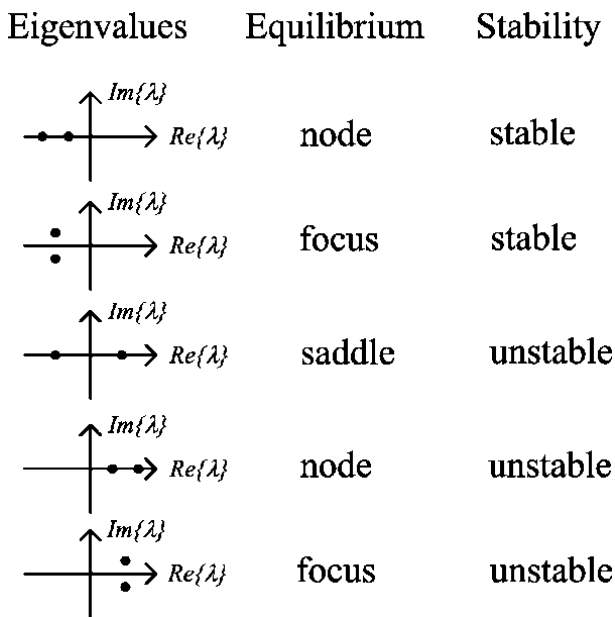


Fig. 7-2. Hyperbolic equilibria of a two-dimensional system.

The solution of Eq. (7.1-6) is derived using Floquet theory [94]

$$\delta \mathbf{x}(t) = \sum_{i=1}^N c_i m_i^{\frac{t}{T}} \mathbf{p}_i(t) = \sum_{i=1}^N c_i e^{\lambda_i t} \mathbf{p}_i(t) \quad (7.1-10)$$

where m_i are the Floquet multipliers and $\mathbf{p}_i(t)$ are periodic vector functions. The Floquet exponents λ_i are related to the multipliers by

$$m_i = e^{\lambda_i T} \quad (7.1-11)$$

It is seen from Eq. (7.1-11) that there is not a unique mapping between multipliers and exponents, as adding to any exponent a complex factor $jk 2\pi/T$ with k an arbitrary integer results in the same multiplier.

The stability of $\mathbf{x}_o(t)$ is determined by the Floquet multipliers m_i . They can be calculated by direct integration of Eq. (7.1-9) for one period T with initial condition $\delta \mathbf{x}(0) = \mathbf{I}_N$ where \mathbf{I}_N is the identity diagonal square matrix of dimension N . The result of the integration is the monodromy matrix \mathbf{C} whose eigenvalues are the desired Floquet multipliers m_i [94].

A periodic solution $\mathbf{x}_o(t)$ of an autonomous system has at least one Floquet multiplier with magnitude equal to 1, or equivalently a Floquet exponent equal to zero. Furthermore, a periodic solution $\mathbf{x}_o(t)$ is stable if the remaining multipliers have a magnitude less than one ($|m_i| < 1$). Correspondingly, if one multiplier with magnitude larger than 1 exists, the solution is unstable.

7.1.4 Lyapunov Exponents

The Lyapunov exponents are defined as follows

$$\mu_i = \lim_{t \rightarrow \infty} \frac{1}{t} \ln |e^{\lambda_i t}| \quad (7.1-12)$$

and can be considered a generalization of both the characteristic eigenvalues of the equilibrium point and the Floquet multipliers of the periodic steady state [101]. In fact, the Lyapunov exponents can be used to determine the stability of quasi-periodic and chaotic steady-state solutions.

One can easily see from Eq. (7.1-7) that the Lyapunov exponents of the equilibrium point correspond to the real part of the characteristic eigenvalues.

$$\mu_{i,eq} = Re\{\lambda_i\} \quad (7.1-13)$$

Correspondingly the Lyapunov exponents of the periodic steady state are equal to the natural logarithm of the magnitude of the Floquet multipliers divided by

the period of the solution which is equal to the real part of the Floquet exponents.

$$\mu_{i,pss} = \frac{\ln|m_i|}{T} = \text{Re}\{\lambda_i\} \quad (7.1-14)$$

7.2 Bifurcations of Nonlinear Dynamical Systems

A dynamical system described by Eq. (7.1-1), in practice depends on a set of parameters ξ of dimension k ($\xi \in \mathbb{R}^k$) which enter the definition of the vector field

$$\dot{x} = f(x, \xi) \quad (7.2-1)$$

A parameter corresponds to some circuit control voltage or bias voltage/current or any other physical parameter such as the dimension of a transmission line. As the parameter vector varies, the solutions of Eq. (7.2-1) change. The change of stability of a specific steady-state solution, the creation of new steady-state solutions or elimination of existing ones, as one or more parameters of a nonlinear system vary is called a *bifurcation* [100,102]. The corresponding parameter values for which a bifurcation occurs are called *bifurcation values*. A *bifurcation diagram* is a plot of a selected state variable(s) corresponding to a limit set versus the system parameter(s). An example of a bifurcation diagram is the plot of the DC voltage at a selected circuit node or the oscillation amplitude versus the external bias voltage of the oscillator. Bifurcations are classified into *local* and *global*. Local bifurcations are detected by studying the vector field f in a neighborhood of a limit set. In contrast, local information is not sufficient to detect global bifurcations. Typically in this book we study systems where one parameter is varied ($k = 1$).

7.2.1 Bifurcations of Equilibrium Points

Let us consider such a continuous time system with one parameter that has a hyperbolic equilibrium point. As the parameter varies, there are two ways that a hyperbolic point can become non-hyperbolic. In the first one, a simple real eigenvalue becomes zero ($\lambda_1 = 0$). In this case the system is going through a bifurcation known as *fold* bifurcation. Fold bifurcation is also known as *turning-point* or *saddle-node* bifurcation. In a fold bifurcation the equilibrium point curve presents an infinite slope at the parameter value $\xi = \xi_0$ where one real eigenvalue becomes zero. This is seen in the bifurcation diagram of a one-dimensional system shown in Fig. 7-3.

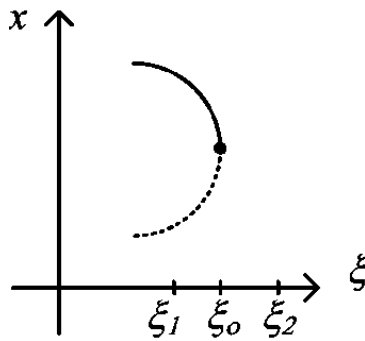


Fig. 7-3. Fold bifurcation.

The infinite slope at ξ_0 corresponding to a real zero eigenvalue leads to a folding, a turning point of the solution curve. For larger values of the parameter $\xi > \xi_0$ no solutions exist, whereas for $\xi < \xi_0$ two solutions exist. In fact, one solution branch contains stable nodes indicated by a solid line, whereas the other unstable (saddle) solutions, and this is indicated by a dotted line [102]. In the case of a one-dimensional system, the unstable solution is a node, whereas in the general case it is a saddle. At the critical value $\xi = \xi_0$, the node and saddle collide, hence the name saddle-node bifurcation.

In the second case, a pair of simple complex eigenvalues fall on the imaginary axis ($\lambda_0 = \pm j\omega_0$ with $\omega_0 > 0$). In this case, the system undergoes a *Hopf* bifurcation, and a limit cycle is born or is extinguished. It is straightforward to see that a Hopf bifurcation requires that the system be at least second order ($n \geq 2$).

An example of a Hopf bifurcation in a two-dimensional system is shown in Fig. 7-4. In a supercritical Hopf bifurcation (Fig. 7-4 a), a stable limit cycle is born as the parameter goes through the bifurcation value ξ_0 . At the same time the stable equilibrium solution becomes unstable. In subcritical Hopf bifurcation (Fig. 7-4 b), an unstable limit cycle is created while an unstable equilibrium point becomes stable.

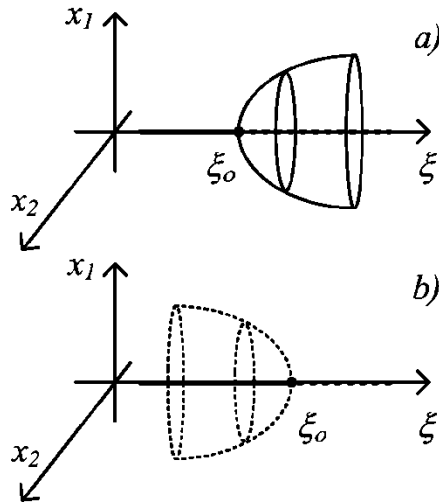


Fig. 7-4. Hopf bifurcation, a) supercritical, b) subcritical.

7.2.2 Bifurcations of Periodic Orbits

Correspondingly, a hyperbolic limit cycle is a limit cycle that does not have any Floquet multipliers with magnitude equal to one [102]. A periodic steady state of an autonomous system has one Floquet multiplier equal to one, and therefore, it is hyperbolic if the remaining multipliers do not have magnitude equal to one.

Given a periodic steady state with frequency $\omega = 2\pi/T$, there exist three types of bifurcations for one-parameter systems [102], corresponding to three distinct possibilities that a multiplier crosses the unit cycle as the parameter is varied, shown in Fig. 7-5.

In the *fold* bifurcation (Fig. 7-5 a), a real multiplier takes the value $m = 1$. In this case the frequency of the limit cycle remains the same, something that can be inferred from Fig. 7-5 a) and Eq. (7.1-10), which describes the linear perturbation of the dynamical system around the periodic steady state. A Floquet multiplier equal to 1 leads to a perturbation that evolves as

$$\delta x(t) = ce^{j\omega t} p(t) \tag{7.2-2}$$

with n integer and therefore it does not perturb the oscillation frequency of the system. A fold bifurcation leads to a change in the stability of the periodic steady-state solution, much as the fold bifurcation of an equilibrium point does for the equilibrium point.

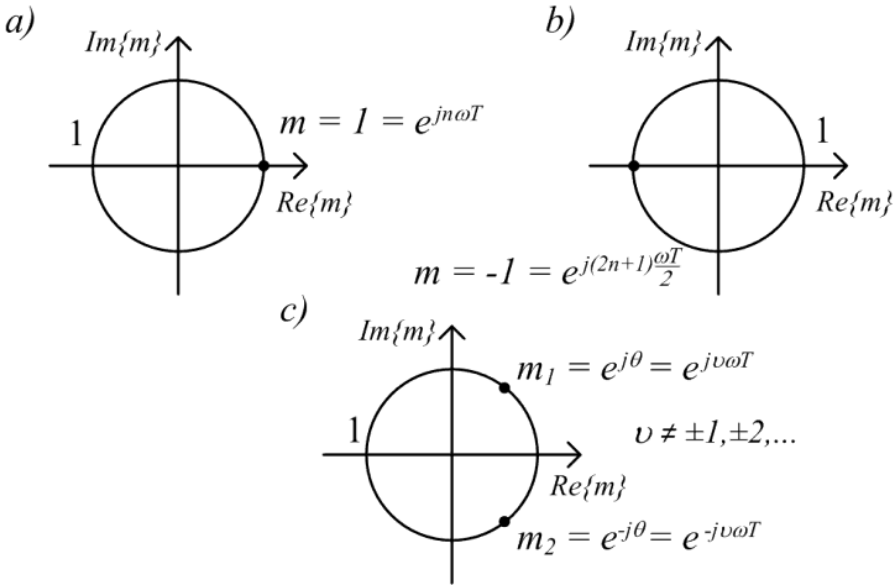


Fig. 7-5. Bifurcations of periodic orbits, a) fold, b) flip, and c) Neimark-Sacker bifurcation.

A *flip* bifurcation occurs when the multiplier becomes $m = -1$ (Fig. 7-5 b). In contrast to the fold bifurcation a flip bifurcation leads to the existence of a new limit cycle whose oscillation frequency is half of the original one. Due to this fact, a flip bifurcation is also known as a *period-doubling* bifurcation. The contribution to the linear variational equation of the $m = -1$ multiplier is

$$\delta x(t) = ce^{j\frac{\omega}{2}t} p(t) \tag{7.2-3}$$

where one can observe the appearance of a term with a frequency half of the original one.

Finally, in a *Neimark-Sacker* or *torus* bifurcation, a pair of complex conjugate multipliers appear on the unit cycle (Fig. 7-5 c). As a result a new frequency, which is not harmonically related to the original one, appears in the system, leading to the onset of a quasi-periodic solution. The contribution to the linear variational equation of this Floquet multiplier is expressed as

$$\delta x(t) = ce^{j\nu\omega t} p(t) \tag{7.2-4}$$

where ν is not an integer.

7.3 The Averaging Method and Multiple Time Scales

The averaging method is typically used to analyze the periodic steady-state solutions of weakly nonlinear systems

$$\dot{\mathbf{x}} = \varepsilon \mathbf{f}(\mathbf{x}, \varepsilon) \quad (7.3-1)$$

and perturbations of the linear oscillator systems [103] [100], with $\varepsilon \ll 1$. It was originally developed by Krylov and Bogoliubov [104]. The method is particularly suitable to analyze the perturbed linear oscillator problem described by

$$\ddot{x} + \omega^2 x = \varepsilon f(x) \quad (7.3-2)$$

where $\omega, x, f \in \mathbb{R}$. The van der Pol differential equation belongs to this class of systems with $f(x) = (1 - x^2)\dot{x}$. In the case of weakly coupled oscillators, an equation of the form Eq. (7.3-2) is used to describe each oscillator, and $f(x)$ contains the nonlinear term of the free-running (uncoupled) oscillator as well as contributions from external coupled signals from other oscillators, which can be linear or nonlinear. The averaging theorem [100] Uc585947 states that there exists a change of coordinates $\mathbf{x} = \mathbf{y} + \varepsilon \mathbf{w}(\mathbf{y}, \varepsilon)$ which transforms Eq. (7.3-1) to the averaged system

$$\dot{\mathbf{y}} = \varepsilon \bar{\mathbf{f}}(\mathbf{y}) \quad (7.3-3)$$

where

$$\bar{\mathbf{f}}(\mathbf{y}) = \frac{1}{2\pi} \int_0^{2\pi} \mathbf{f}(\mathbf{y}(z), 0) dz \quad (7.3-4)$$

The system given by Eq. (7.3-3) is an autonomous system, whereas Eq. (7.3-1) can be non-autonomous. The essential property of the averaged system that is extensively applied in the study of coupled oscillator systems is that a hyperbolic periodic steady state of Eq. (7.3-3) corresponds to a hyperbolic equilibrium point of Eq. (7.3-1) and that both steady states have the same stability [100]. This essentially means that the eigenvalues of the linearized system of an equilibrium point of Eq. (7.3-3) determine its stability. This is quite useful as obtaining the Floquet multipliers of a microwave oscillator may not be a trivial task. Furthermore, for the cases that are considered in this book, the bifurcations of the averaged system are the same as those of the original system [100].

In order to transform the perturbed linear oscillator problem in the standard form Eq. (7.3-1), the following transformation (known as the van der Pol transformation [100] [103]) is commonly applied to Eq. (7.3-2) before averaging,

$$x = A \cos(\omega t + \phi) \tag{7.3-5}$$

$$\dot{x} = -\omega A \sin(\omega t + \phi)$$

In this case Eq. (7.3-2) becomes

$$\dot{A} \approx -\frac{\varepsilon}{\omega} \sin(\omega t + \phi) f(A, \phi, \varepsilon) = \varepsilon g_1(A, \phi, \varepsilon) \tag{7.3-6}$$

$$\dot{\phi} \approx -\frac{\varepsilon}{A\omega} \cos(\omega t + \phi) f(A, \phi, \varepsilon) = \varepsilon g_2(A, \phi, \varepsilon)$$

Applying Eq. (7.3-4), the averaged solution is obtained

$$\dot{\bar{A}} = \varepsilon \bar{g}_1(\bar{A}, \bar{\phi}) \tag{7.3-7}$$

$$\dot{\bar{\phi}} = \varepsilon \bar{g}_2(\bar{A}, \bar{\phi})$$

It should be noted that the transformation given by Eq. (7.3-5) and subsequent application of the perturbation method limits the analysis of the system given by Eq. (7.3-2) locally near the oscillation frequency ω in the frequency domain. The system can be studied near a different harmonic by modifying appropriately the transformation, that is, setting $n\omega$ in place of ω where n is the desired harmonic order. In practice, considering the oscillator behavior near the fundamental frequency is sufficient for the study of high Q oscillators because higher harmonics are small and therefore can be ignored in the analysis. Specifically, the averaged Van der Pol differential equation for which $f(x) = (1 - x^2)\dot{x}$ becomes [103]

$$\dot{\bar{A}} = \frac{\varepsilon}{2} \bar{A} \left(1 - \frac{\bar{A}^2}{4} \right) \tag{7.3-8}$$

$$\dot{\bar{\phi}} = 0$$

The above system leads to a nontrivial steady-state oscillation with amplitude $\bar{A} = 2$ obtained by requiring that $\dot{\bar{A}} = 0$.

7.4 Averaging Theory in Coupled Oscillator Systems

Kurokawa considered the oscillator equivalent of a series resistance, inductance, capacitance (RLC) resonator connected in series with a negative resistance and applied the averaging theory to study the properties of noisy oscillators and injection locked oscillators [105].

The theory of Kurokawa applied to the study of coupled oscillator arrays was introduced to the antennas and microwaves communities by Stephan [1] with an aim towards antenna-array applications such as power-combining arrays and phased arrays. The work of Stephan focused on taking advantage of the dynamical properties of coupled oscillator array topologies in order to generate constant phase shift distributions among the array elements in a continuously variable manner. A parallel RLC resonator in parallel with a negative resistance was used to model each oscillator, leading to a dual form of the one used by Kurokawa.

It should be noted that there is significant theoretical work in the literature regarding coupled oscillator systems, also called distributed and ladder oscillators, considering the various operating modes and stability of one- and two-dimensional arrays. Notable references are [106] [107] [108] [109]. The latter work by Endo and Mori [109] presented an elegant way to obtain a formulation equivalent to a perturbed van der Pol equation in vector form for an array of coupled oscillators modeled as a parallel RLC resonator with a negative resistance, and it will be given in the next section. An efficient analysis of coupled oscillator arrays for quasi-optical power combining and the stability of the various existing operating modes was proposed by York and Compton [110] utilizing only the phase dynamics of the array, or in other words the second equation of Eq. (7.3-7).

We may distinguish among power-combining applications where the stability of the various operating modes of coupled oscillator systems is with an aim to secure excitation of only the in-phase mode, and applications where an arbitrary phase distribution among the oscillator elements is required (such as beamforming and phased arrays). The latter may be viewed as a generalization of the former.

Following their initial work, York produced a general formulation for coupled-oscillator arrays based on the fundamental harmonic approximation and the averaging method that is essentially used to date in most approximate analysis methods for such systems [111], [95]. Furthermore, York introduced an elegant way to achieve constant progressive phase shifts among the array oscillator elements in a continuous fashion by only modifying the oscillation frequency of the end elements of the array. In 2004, Heath presented an elegant and unifying formulation of the application of the method of averaging (specifically the Lindstedt method was used to derive the slow time differential equations [94]) in coupled-oscillator arrays along with a detailed stability analysis of various different coupling network topologies [112]. The latter formulation is given here

$$\begin{aligned} \dot{A}_m = \mu(A_{om}^2 - A_m^2)A_m \\ + \sum_{i=1}^N K_{mi}A_i \cos(\phi_i - \phi_m + \Phi_{im}) \end{aligned} \quad (7.4-1)$$

$$\begin{aligned} A_m \dot{\phi}_m = \Delta\omega_m A_m \\ + \sum_{i=1}^N K_{mi}A_i \sin(\phi_i - \phi_m + \Phi_{im}) \end{aligned}$$

where an array of N oscillators is assumed. The variable A_m represents the slowly varying averaged amplitude of oscillator m , as given in Eq. (7.3-7) with the bar suppressed for simplicity. Correspondingly, the phase of oscillator m is given by $\theta_m = \omega_o t + \phi_m$ where ϕ_m is the averaged time varying component of the oscillator phase corresponding to Eq. (7.3-7) (with the bar suppressed). When uncoupled to the rest of the array elements, each oscillator m has a periodic steady state with amplitude A_{om} and frequency $\omega_m = \omega_o + \Delta\omega_m$. Furthermore, each individual oscillator satisfies a van der Pol differential equation of nonlinearity constant ε , which appears in Eq. (7.4-1) through $\mu = \varepsilon \omega_m / (2Q)$ where Q is the external quality factor of the resonator of each oscillator element calculated using a reference load admittance G_L . Coupling among the oscillator elements is included in the form of a square complex matrix $T = [t_{mi}]$ of dimension N , with $t_{mi} = T_{mi} e^{j\Phi_{mi}}$. Note that T is a transfer function (unitless). If for example an admittance matrix is used to express the coupling among oscillator elements, then T is the admittance matrix normalized to the reference load admittance G_L . In Eq. (7.4-1) the coupling coefficients also appear in normalized form setting

$$\kappa = [\kappa_{mi}] = [K_{mi} e^{j\Phi_{mi}}] = [t_{mi} \omega_m / 2Q] \quad (7.4-2)$$

Finally, Eq. (7.4-1) can be written in a complex valued compact format letting $\alpha_m = A_m e^{j\phi_m}$

$$\dot{\alpha}_m = j\Delta\omega_m \alpha_m + \mu(A_{om}^2 - |\alpha_m|^2)\alpha_m + \sum_{i=1}^N \kappa_{mi} \alpha_i \quad (7.4-3)$$

Under weak coupling conditions, the phase dynamics alone are sufficient to analyze the behavior of the coupled oscillator system. We may then consider only the second equation of Eq. (7.4-1) and assume that the oscillator amplitudes are approximately equal to their uncoupled values $A_m = A_o$. The system of equations pertaining to the phase dynamics provide significant insight and a very computationally efficient method to analyze arrays with a

large number of elements. In fact, the analysis results of Part I of this book have focused on the phase dynamics of coupled oscillator arrays. The system of equations limited to the phase dynamics was introduced as the “generalized phase model” by Heath in [112]:

$$\dot{\phi}_m = \Delta\omega_m + \sum_{i=1}^N K_{mi} \sin(\phi_i - \phi_m + \Phi_{mi}) \quad (7.4-4)$$

When no coupling phase Φ_{mi} is considered, the model is the well known Kuramoto model [113]. In the special case where a bi-directional symmetrical coupling matrix with $\kappa_{im} = \kappa_{mi}$ is considered, the generalized phase model coincides with the phase model introduced by York in [111].

A fixed point of Eq. (7.4-1) corresponds to a periodic steady-state solution, defined for $\dot{A}_m = 0$ and $\dot{\phi}_m = c$ with c an arbitrary constant. Letting c take nonzero values still corresponds to synchronized solutions of the array but for a different frequency than ω_o .

$$\begin{aligned} \mu(A_{om}^2 - A_m^2)A_m + \sum_{i=1}^N K_{mi}A_i \cos(\phi_i - \phi_m + \Phi_{im}) \\ = 0 \end{aligned} \quad (7.4-5)$$

$$\begin{aligned} (\Delta\omega_m - c)A_m + \sum_{i=1}^N K_{mi}A_i \sin(\phi_i - \phi_m + \Phi_{im}) \\ = 0 \end{aligned}$$

Every set (A_m, ϕ_m) that satisfies the above conditions corresponds to an oscillating mode of the array. In principle there exist up to 2^{N-1} modes [111]. It should be emphasized that, due to the autonomous nature of the coupled oscillator system, it is possible to translate all oscillator phases ϕ_m by the same arbitrarily large value and still obtain the same steady-state solution. This is evidenced by the fact that only phase differences appear in Eq. (7.4-5). In other words, the steady state is defined by the oscillator phase differences and not their absolute phase.

The stability of the oscillating modes is examined by considering the linear perturbation $(A_m + \delta A_m, \phi_m + \delta \phi_m)$ of Eq. (7.4-1), which leads to a system of linear differential equations

$$\begin{aligned}
 \delta \dot{A}_m &= \mu(A_{\delta m}^2 - 3A_m^2)\delta A_m \\
 &+ \sum_{i=1}^N K_{mi} \cos(\phi_i - \phi_m + \Phi_{mi}) \delta A_i \\
 &- \sum_{i=1}^N K_{mi} A_i \sin(\phi_i - \phi_m + \Phi_{mi}) (\delta \phi_i \\
 &- \delta \phi_m)
 \end{aligned} \tag{7.4-6}$$

$$\begin{aligned}
 A_m \delta \dot{\phi}_m &= -\dot{\phi}_m \delta A_m + \sum_{i=1}^N K_{mi} \sin(\phi_i - \phi_m + \Phi_{mi}) \delta A_i \\
 &+ \sum_{i=1}^N K_{mi} A_i \cos(\phi_i - \phi_m + \Phi_{mi}) (\delta \phi_i \\
 &- \delta \phi_m)
 \end{aligned}$$

In the case of the generalized phase model one has

$$\delta \dot{\phi}_m = \sum_{i=1}^N K_{mi} \cos(\phi_i - \phi_m + \Phi_{mi}) (\delta \phi_i - \delta \phi_m) \tag{7.4-7}$$

Because the steady state is defined by phase differences and not absolute phase values, the perturbation phase values $\delta \phi_m$ of the steady state may not be small. Their differences, however, are assumed to be small, and this allows one to take the linear approximation of the cosine and sine terms in Eq. (7.4-1) and obtain Eq. (7.4-6).

7.5 Obtaining the Parameters of the van der Pol Oscillator Model

A useful analytical method is presented, that allows one to obtain the van der Pol differential equation from a parallel resonator with a nonlinear voltage dependent current source. The procedure follows the development presented by Endo and Mori in [108], and it represents a time-domain formulation of van der Pol's model described in Section 1.2. This model has very low complexity, and it can be easily incorporated into analysis of large arrays or proof of concept for various topologies of coupled oscillators. In addition, it can be easily introduced into circuit simulators.

Given a nonlinear voltage dependent current source $i_n = f(v)$ with time derivative $di/dt = g_v(v)\dot{v}$, where $g_v(v) = df(v)/dv$ is a nonlinear conductance and applying Kirchoff's current law in the circuit of Fig. 7-6, one has

$$C\dot{v} + g_L v + \frac{1}{L}i_1 + i_n + i_{inj} = 0 \tag{7.5-1}$$

which, after differentiating becomes

$$C\ddot{v} + (g_L + g_v)\dot{v} + \frac{v}{L} + i_{inj} = 0 \tag{7.5-2}$$

Defining the natural frequency of the tank $\omega_o^2 = 1/LC$, setting $\varepsilon = g_L/(C\omega_o)$ and scaling time $t = \omega_o\tau$ the differential equation takes the form

$$v'' + \varepsilon\left(1 + \frac{g_v}{g_L}\right)v' + v + \frac{\varepsilon}{g_L}i'_{inj} = 0 \tag{7.5-3}$$

where ()' indicates the scaled time derivative $d/d\tau$.

If we consider a nonlinear current source modeled by a third order polynomial, the equation corresponding to the free-running oscillator ($i_{inj} = 0$) can be transformed to the van der Pol equation. Let a voltage-dependent current source be of the form

$$i_n = f(v) = -g_1v + g_3v^3 \tag{7.5-4}$$

so that

$$g_v(v) = -g_1 + 3g_3v^2 \tag{7.5-5}$$

Setting

$$\lambda = \varepsilon \frac{g_1 - g_L}{g_L} = \frac{g_1 - g_L}{C\omega_o} = \frac{1}{Q} \tag{7.5-6}$$

one obtains:

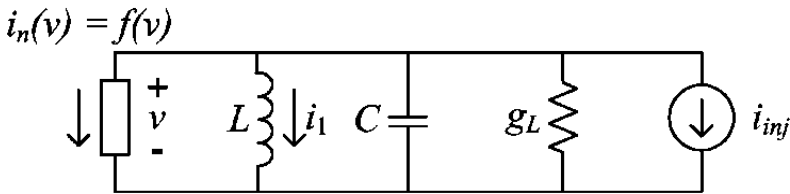


Fig. 7-6. Oscillator model consisting of a parallel RLC resonator and a nonlinear voltage dependent current source.

$$v'' - \lambda \left(1 - \frac{3g_3}{g_1 - g_L} v^2\right) v' + v + \frac{\lambda}{g_1 - g_L} i'_{inj} = 0 \quad (7.5-7)$$

The parameter λ is equal to the inverse of the loaded quality factor, Q , of the oscillator circuit of Fig. 7-6.

Finally, scaling the voltage as

$$x = \sqrt{\beta} v = \sqrt{\frac{3g_3}{g_1 - g_L}} v \quad (7.5-8)$$

the differential equation takes the desired form:

$$x'' - \lambda(1 - x^2)x' + x + \lambda \sqrt{\frac{3g_3}{(g_1 - g_L)^3}} i'_{inj} = 0 \quad (7.5-9)$$

When no injection signal is present, $i_{inj} = 0$, and this equation becomes the well known van der Pol equation.

$$x'' - \lambda(1 - x^2)x' + x = 0 \quad (7.5-10)$$

The approximate solution to the van der Pol oscillation is [94]

$$x = 2 \cos \tau \Rightarrow v = \frac{2}{\sqrt{\beta}} \sin \omega_o t \quad (7.5-11)$$

which is identical to the solution provided by the averaging method in Section 7.3.

The approximate parallel model for the oscillator can be extracted using a nonlinear simulator and calculating the admittance at a selected circuit node [114]. Several authors have proposed experimental techniques to evaluate the model parameters [114,115]. Measurement of the oscillator amplitude can be used to obtain the scaling parameter β . Injection locking the oscillator to an external signal and measuring the locking bandwidth can be used to estimate the Q and subsequently the second parameter λ of the van der Pol model [114]. Alternatively, a low-frequency sinusoidal modulating signal can be introduced in the bias circuitry of the oscillator, resulting in a phase modulated oscillator output. The parameter λ can then be obtained by measuring the relative amplitude of the modulation sidebands [115].

7.6 An Alternative Perturbation Model for Coupled-Oscillator Systems

It is possible to formulate an alternative practical model for analyzing coupled oscillator arrays by considering that the periodic steady state of the coupled system is a perturbation of the free running steady state of the individual oscillator elements when they are uncoupled to each other. This assumption holds when the coupling is weak, as is typically the case when designing such systems. The model described in this section was proposed in Ref. [116].

An advantage of this formulation is that there is no underlying assumption about the oscillator nonlinearity model, such as for example a third-order nonlinearity used in the van der Pol model, and each individual oscillator can be designed using any numerical technique. The uncoupled free-running steady state is expressed in the slow time (at the fundamental frequency component) as

$$Y_o(V, \omega, \mu)V_oe^{j\phi_o} = 0 \tag{7.6-1}$$

where Y_o is the admittance looking into a properly selected node of the circuit and V_o the oscillation amplitude at that node (Fig. 7-7).

This is merely application of Kirchhoff’s current law at the node under consideration. Y_o typically contains both linear and nonlinear terms, and depends on the oscillation frequency $\omega = \omega_o$ and amplitude $V = V_o$. Generally, one may assume that Y_o depends on a number of additional circuit parameters, such as bias voltages. In Eq. (7.6-1) a single parameter $\mu = \mu_o$ is considered which corresponds to some DC voltage that allows for frequency tuning. Assuming a nonzero periodic steady-state amplitude V_o , Eq. (7.6-1) is satisfied for $Y_o = 0$. A free-running oscillator is an autonomous system characterized by an arbitrary time reference, which translates in an arbitrary phase reference in the frequency domain. As a result $\phi_o = 0$ maybe set without loss of generality.

A coupled oscillator array of N elements is then described by

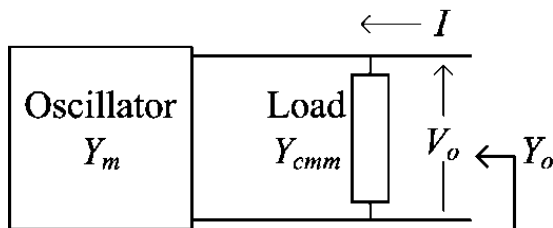


Fig. 7-7. Oscillator 1-port equivalent circuit.

$$Y_m V_m e^{j\phi_m} + \sum_{i=1}^N Y_{cmi} V_i e^{j\phi_i} = 0 \tag{7.6-2}$$

where the coupling is represented by the admittance matrix $Y_c(\omega) = [Y_{cmi}(\omega)]$ which typically is frequency dependent. The coupling results in a steady state that can be expressed as a perturbation of the individual oscillator free-running steady state as follows:

$$V_m = V_o + \Delta V_m(t) \tag{7.6-3}$$

$$\phi_m = \phi_{om} + \Delta\phi_m(t)$$

$$\mu_m = \mu_{om} + \Delta\mu_m$$

$$\omega = \omega_o + \dot{\phi}_m(t) - \frac{j\dot{V}_m}{V_m}$$

$$Y_{cmi}(\omega) = Y_{cmi}(\omega_o) + \frac{\partial Y_{cmi}}{\partial \omega_o}(\omega - \omega_o)$$

$$Y_m(V, \omega, \mu) = \frac{\partial Y_m}{\partial V_o}(V_m - V_o) + \frac{\partial Y_m}{\partial \omega_o}(\omega - \omega_o) + \frac{\partial Y_m}{\partial \mu_o}(\mu_m - \mu_o)$$

The perturbation assumption has been used in the first place by York, Liao, and Lynch [33], and it is described in Section 1.3 dealing with the injection-locked oscillator. However, in their analysis they proceed to assume a specific nonlinear dependence of the admittance on the amplitude V_m whereas here no such assumption is made. Furthermore, it should be noted that the frequency expansion has been done using the well known Kurokawa transformation [105] introduced in Section 1.3. The commonly used coupling networks have a broadband frequency response relative to the oscillator locking bandwidth, which allows us to consider a constant coupling term $Y_{cmi}(\omega) = Y_{cmi}(\omega_o)$. Narrowband coupling networks were studied by Lynch and York [117]. After some straightforward manipulation, one obtains

$$\begin{aligned}
\frac{\partial Y_m}{\partial \omega_o} [-j\dot{V}_m + V_m \dot{\phi}_m] + \frac{\partial Y_m}{\partial \mu_o} \Delta \mu_m V_m \\
+ \frac{\partial Y_m}{\partial V_o} (V_m - V_o) V_m \\
+ \sum_{i=1}^N Y_{cmi}(\omega_o) V_i e^{j(\phi_i - \phi_m)} = 0
\end{aligned} \tag{7.6-4}$$

This system of differential equations represents the basis for an alternative model formulation for a system of coupled oscillators. This formulation has been essentially introduced in Ref. [116] and refined in Ref. [118] as well as subsequent works as a basis to study several properties of coupled oscillator arrays.

In order to appreciate the similarities and differences with the original model of Section 7.4, the amplitude and phase equations are decoupled by first dividing with $\partial Y_m / \partial \omega_o$ and then considering real and imaginary parts. Let for simplicity

$$C_V = j \frac{\partial Y^{-1}}{\partial \omega_o} \frac{\partial Y}{\partial V_o} = C_V^R + jC_V^I \tag{7.6-5}$$

$$C_\mu = j \frac{\partial Y^{-1}}{\partial \omega_o} \frac{\partial Y}{\partial \mu_o} = C_\mu^R + jC_\mu^I$$

$$\begin{aligned}
C_c = [C_{cmi}] &= \left[j \frac{\partial Y^{-1}}{\partial \omega_o} Y_{mi}(\omega_o) \right] = [|C_{cmi}| e^{j\psi_{mi}}] \\
&= [C_{cmi}^R + jC_{cmi}^I]
\end{aligned}$$

Using the above, Eq. (7.6-4) becomes

$$\begin{aligned}
\dot{V}_m + C_V^R (V_m - V_o) V_m + C_\mu^R \Delta \mu_m V_m \\
+ \sum_{i=1}^N |C_{cmi}| V_i \cos(\phi_{oi} - \phi_{om} + \psi_{mi}) \\
= 0
\end{aligned} \tag{7.6-6}$$

$$\begin{aligned}
 V_m \dot{\phi}_m + C_V^I (V_m - V_o) V_m + C_\mu^I \Delta\mu_m V_m \\
 + \sum_{i=1}^N |C_{cmi}| V_i \sin(\phi_{oi} - \phi_{om} + \Psi_{mi}) \\
 = 0
 \end{aligned}$$

Furthermore, letting $v_m = V_m e^{j\phi_m}$ it is possible to express Eq. (7.6-6) in a compact complex form

$$\dot{v}_m + C_V (|v_m| - V_o) v_m + C_\mu \Delta\mu_m v_m + \sum_{i=1}^N C_{cmi} v_i = 0 \quad (7.6-7)$$

The corresponding generalized phase model associated with this formulation is obtained considering only the phase dynamics which results in

$$\dot{\phi}_m + C_\mu^I \Delta\mu_m + \sum_{i=1}^N |C_{cmi}| \sin(\phi_{oi} - \phi_{om} + \Psi_{mi}) = 0 \quad (7.6-8)$$

The periodic steady-state solution is obtained by setting $\dot{V}_m = 0$ and $\dot{\phi}_m = \Delta\omega$ leading to

$$\begin{aligned}
 C_V^R (V_m - V_o) V_m + C_\mu^R \Delta\mu_m V_m \\
 + \sum_{i=1}^N |C_{cmi}| V_i \cos(\phi_{oi} - \phi_{om} + \Psi_{mi}) \\
 = 0
 \end{aligned} \quad (7.6-9)$$

$$\begin{aligned}
 V_m \Delta\omega + C_V^I (V_m - V_o) V_m + C_\mu^I \Delta\mu_m V_m \\
 + \sum_{i=1}^N |C_{cmi}| V_i \sin(\phi_{oi} - \phi_{om} + \Psi_{mi}) \\
 = 0
 \end{aligned}$$

or in complex notation

$$\begin{aligned}
 C_V (V_m - V_o) V_m + j V_m \Delta\omega + C_\mu \Delta\mu_m V_m \\
 + \sum_{i=1}^N C_{cmi} V_i e^{j(\phi_{oi} - \phi_{om})} = 0
 \end{aligned} \quad (7.6-10)$$

As was the case with the model represented by Eq. (7.4-1) the steady state of the array is defined by phase differences and not absolute phases. In order to study the stability of the steady-state solution, we form the linear perturbation of Eq. (7.6-4) using $(V_m + \delta V_m, \phi_m + \delta \phi_m)$, where small-amplitude perturbations δV_m and small-phase perturbation differences $(\delta \phi_m - \delta \phi_i)$ are considered leading to

$$\begin{aligned} \delta \dot{V}_m + [C_V^R(2V_m - V_o) + C_\mu^R(\mu_m - \mu_o)]\delta V_m \\ + \sum_{i=1}^N |C_{cmi}| \cos(\phi_{oi} - \phi_{om} + \Psi_{mi}) \delta V_i \\ - \sum_{i=1}^N |C_{cmi}| V_i \sin(\phi_{oi} - \phi_{om} + \Psi_{mi}) (\delta \phi_i \\ - \delta \phi_m) = 0 \end{aligned} \quad (7.6-11)$$

$$\begin{aligned} V_m \delta \dot{\phi}_m + [\Delta\omega + C_V^I(2V_m - V_o) + C_\mu^I(\mu_m - \mu_o)]\delta V_m \\ + \sum_{i=1}^N |C_{cmi}| \sin(\phi_{oi} - \phi_{om} + \Psi_{mi}) \delta V_i \\ + \sum_{i=1}^N |C_{cmi}| V_i \cos(\phi_{oi} - \phi_{om} + \Psi_{mi}) (\delta \phi_i \\ - \delta \phi_m) = 0 \end{aligned}$$

Correspondingly, the generalized phase model stability is then determined by

$$\delta \dot{\phi}_m + \sum_{i=1}^N |C_{cmi}| \cos(\phi_{oi} - \phi_{om} + \Psi_{mi}) (\delta \phi_i - \delta \phi_m) = 0 \quad (7.6-12)$$

The eigenvalues of the linear variational equation determine the stability of the steady-state solutions. In practice, it is more computationally efficient to formulate and process the array equations as matrix equations, and this is the topic of the next section.

7.7 Matrix Equations for the Steady State and Stability Analysis

It is easier from a computational point of view to express the various systems of equations of the previous sections in matrix form. In order to do so, the

following notation and properties are used. Bold letterface indicates a column vector or a matrix. The dimension of the vector or square matrix is N unless noted otherwise, $\mathbf{0}$ and $\mathbf{1}$ indicate a vector of zeros and a vector of ones, respectively. The notation $[a_m]$ and $[a_{mi}]$ define a vector and a matrix α , respectively. The function $\text{dg}(\cdot)$ converts a vector to a square diagonal matrix of size N . It is straightforward to show that for any two vectors \mathbf{a} and \mathbf{b} , $\text{dg}(\mathbf{a})\mathbf{b} = \text{dg}(\mathbf{b})\mathbf{a}$. The superscript $(\cdot)^H$ indicates the conjugate transpose of a matrix or vector, whereas superscripts $(\cdot)^R$ and $(\cdot)^I$ indicate real and imaginary part. One can then rewrite Eq. (7.4-1) in matrix form

$$\dot{\mathbf{A}} + j\text{dg}(\mathbf{A})\dot{\boldsymbol{\phi}} = \text{dg}(\mathbf{p}_1(\mathbf{A}) + j\Delta\boldsymbol{\omega})\mathbf{A} + \boldsymbol{\Phi}^H\boldsymbol{\kappa}\boldsymbol{\Phi}\mathbf{A} \quad (7.7-1)$$

where $\boldsymbol{\Phi} = \text{dg}[e^{j\phi_m}]$. The system given by Eq. (7.7-1) can be integrated numerically after separating real and imaginary parts,

$$\begin{bmatrix} \mathbf{I} & \mathbf{0} \\ \mathbf{0} & \text{dg}(\mathbf{A}) \end{bmatrix} \begin{bmatrix} \dot{\mathbf{A}} \\ \dot{\boldsymbol{\phi}} \end{bmatrix} = \begin{bmatrix} \text{dg}(\mathbf{p}_1(\mathbf{A}))\mathbf{A} + (\boldsymbol{\Phi}^H\boldsymbol{\kappa}\boldsymbol{\Phi})^R\mathbf{A} \\ \text{dg}(\Delta\boldsymbol{\omega})\mathbf{A} + (\boldsymbol{\Phi}^H\boldsymbol{\kappa}\boldsymbol{\Phi})^I\mathbf{A} \end{bmatrix} \quad (7.7-2)$$

where the vector function $\mathbf{p}_1(\mathbf{A})$ is defined as $\mathbf{p}_1(\mathbf{A}) = [\mu(A_{om}^2 - A_m^2)]$. The generalized phase model (7.4-4) is then given by

$$\dot{\boldsymbol{\phi}} = \Delta\boldsymbol{\omega} + (\boldsymbol{\Phi}^H\boldsymbol{\kappa}\boldsymbol{\Phi})^I\mathbf{1} \quad (7.7-3)$$

The steady state of Eq. (7.7-2) is computed by setting $\dot{\mathbf{A}} = \mathbf{0}$ and $\dot{\boldsymbol{\phi}} = c\mathbf{1}$ which, when substituted in (7.7-2), result in the trivial solution $\mathbf{A} = \mathbf{0}$ or

$$\begin{bmatrix} \text{dg}(\mathbf{p}_1(\mathbf{A})) + (\boldsymbol{\Phi}^H\boldsymbol{\kappa}\boldsymbol{\Phi})^R \\ \text{dg}(\Delta\boldsymbol{\omega} - c\mathbf{1}) + (\boldsymbol{\Phi}^H\boldsymbol{\kappa}\boldsymbol{\Phi})^I \end{bmatrix} = \begin{bmatrix} \mathbf{0} \\ \mathbf{0} \end{bmatrix} \quad (7.7-4)$$

The linear variational equation of Eq. (7.7-1) is also written as a matrix linear differential equation as follows

$$\delta\dot{\mathbf{A}} + j\text{dg}(\mathbf{A})\delta\dot{\boldsymbol{\phi}} = \mathbf{D}_A\delta\mathbf{A} + \mathbf{D}_\phi\delta\boldsymbol{\phi} \quad (7.7-5)$$

with

$$\mathbf{D}_A = \text{dg}(\mathbf{g}_1(\mathbf{A}) + j(\Delta\boldsymbol{\omega} - c\mathbf{1})) + \boldsymbol{\Phi}^H\boldsymbol{\kappa}\boldsymbol{\Phi} \quad (7.7-6)$$

$$\mathbf{D}_\phi = j[\boldsymbol{\Phi}^H\boldsymbol{\kappa}\boldsymbol{\Phi}\text{dg}(\mathbf{A}) - \text{dg}(\boldsymbol{\Phi}^H\boldsymbol{\kappa}\boldsymbol{\Phi}\mathbf{A})]$$

where $\mathbf{g}_1(\mathbf{A}) = [\mu(A_{om}^2 - 3A_m^2)]$. The complex system of Eq. (7.7-5) is separated into real and imaginary parts as

$$\begin{bmatrix} \mathbf{I} & \mathbf{0} \\ \mathbf{0} & \text{dg}(\mathbf{A}) \end{bmatrix} \begin{bmatrix} \delta\dot{\mathbf{A}} \\ \delta\dot{\boldsymbol{\phi}} \end{bmatrix} = \begin{bmatrix} \mathbf{D}_A^R & \mathbf{D}_\phi^R \\ \mathbf{D}_A^I & \mathbf{D}_\phi^I \end{bmatrix} \begin{bmatrix} \delta\mathbf{A} \\ \delta\boldsymbol{\phi} \end{bmatrix} \quad (7.7-7)$$

or

$$\begin{bmatrix} \delta \dot{A} \\ \delta \dot{\phi} \end{bmatrix} = D \begin{bmatrix} \delta A \\ \delta \phi \end{bmatrix} = \begin{bmatrix} D_A^R & D_\phi^R \\ \text{dg}(A)^{-1} D_A^I & \text{dg}(A)^{-1} D_\phi^I \end{bmatrix} \begin{bmatrix} \delta A \\ \delta \phi \end{bmatrix} \quad (7.7-8)$$

where $\text{dg}(A)^{-1}$ is a diagonal matrix with the inverse of the steady-state oscillator amplitudes in its diagonal. The inversion operation is guaranteed to exist under the assumption that the steady-state solution corresponds to nonzero amplitudes for all oscillators.

Correspondingly, the linear variational equation of the generalized phase model is

$$\delta \dot{\phi} = D_C \delta \phi = [\Phi^H \kappa \Phi - \text{dg}(\Phi^H \kappa \Phi \mathbf{1})]^R \delta \phi \quad (7.7-9)$$

The matrix differential equation pertaining to the coupled-oscillator dynamics according to the alternative model Eq. (7.6-4) becomes

$$\dot{V} + j \text{dg}(V) \dot{\phi} + C_V p_V(V) + C_\mu \text{dg}(V) \Delta \mu + \Phi^H C_c \Phi V = \mathbf{0} \quad (7.7-10)$$

where $p_V(V) = (\text{dg}(V) - V_o I)V$. After separating into real and imaginary parts one obtains

$$\begin{bmatrix} I & \mathbf{0} \\ \mathbf{0} & \text{dg}(V) \end{bmatrix} \begin{bmatrix} \dot{V} \\ \dot{\phi} \end{bmatrix} = \begin{bmatrix} C_V^R p_V(V) + C_\mu^R \text{dg}(V) \Delta \mu + (\Phi^H C_c \Phi)^R V \\ C_V^I p_V(V) + C_\mu^I \text{dg}(V) \Delta \mu + (\Phi^H C_c \Phi)^I V \end{bmatrix} \quad (7.7-11)$$

The steady-state solution is then given by the nonlinear system of algebraic equations

$$\begin{bmatrix} C_V^R p_V(V) + C_\mu^R \text{dg}(V) \Delta \mu + (\Phi^H C_c \Phi)^R V \\ \text{dg}(V) \Delta \omega \mathbf{1} + C_V^I p_V(V) + C_\mu^I \text{dg}(V) \Delta \mu + (\Phi^H C_c \Phi)^I V \end{bmatrix} = \begin{bmatrix} \mathbf{0} \\ \mathbf{0} \end{bmatrix} \quad (7.7-12)$$

Due to the perturbation assumption, one may consider a linear approximation of the steady state as follows

$$\begin{bmatrix} C_V^R I + \frac{1}{V_o} (\Phi^H C_c \Phi)^R & C_\mu^R I \\ C_V^I I + \frac{1}{V_o} (\Phi^H C_c \Phi)^I & C_\mu^I I \end{bmatrix} \begin{bmatrix} \Delta V \\ \Delta \mu \end{bmatrix} + \begin{bmatrix} (\Phi^H C_c \Phi)^R \mathbf{1} \\ \Delta \omega \mathbf{1} + (\Phi^H C_c \Phi)^I \mathbf{1} \end{bmatrix} = \begin{bmatrix} \mathbf{0} \\ \mathbf{0} \end{bmatrix} \quad (7.7-13)$$

For a given frequency offset $\Delta\omega$ and phase distribution along the array elements contained in Φ , one may solve the above linear system of $2N$ equations for the N steady-state oscillator amplitudes and N control perturbations. Alternatively, one may fix the control parameter of one arbitrarily selected oscillator and solve the steady-state system for the N steady-state oscillator amplitudes, $N - 1$ remaining control perturbations and frequency offset $\Delta\omega$.

The stability of the steady-state solution is obtained taking the linear variational equation of Eq. (7.7-10) leading to the following linearized system of differential equations

$$\delta \dot{V} + j \text{dg}(V) \delta \dot{\phi} = D_V \delta V + D_\phi \delta \phi \quad (7.7-14)$$

where

$$D_V = -j \Delta \omega \mathbf{1} - \text{dg}(C_V g_V(V) + C_\mu^R \Delta \mu) - \Phi^H C_c \Phi \quad (7.7-15)$$

$$D_\phi = -j [\Phi^H C_c \Phi \text{dg}(V) - \text{dg}(\Phi^H C_c \Phi V)]$$

where $g_V(V) = 2V - V_o I$. One then separates real from imaginary parts to obtain the desired system of linear differential equations

$$\begin{bmatrix} I & \mathbf{0} \\ \mathbf{0} & \text{dg}(V) \end{bmatrix} \begin{bmatrix} \delta \dot{V} \\ \delta \dot{\phi} \end{bmatrix} = \begin{bmatrix} D_V^R & D_\phi^R \\ D_V^I & D_\phi^I \end{bmatrix} \begin{bmatrix} \delta V \\ \delta \phi \end{bmatrix} \quad (7.7-16)$$

or

$$\begin{bmatrix} \delta \dot{V} \\ \delta \dot{\phi} \end{bmatrix} = K \begin{bmatrix} \delta V \\ \delta \phi \end{bmatrix} = \begin{bmatrix} D_V^R & D_\phi^R \\ \text{dg}(V)^{-1} D_V^I & \text{dg}(V)^{-1} D_\phi^I \end{bmatrix} \begin{bmatrix} \delta V \\ \delta \phi \end{bmatrix} \quad (7.7-17)$$

The $2N$ eigenvalues of the square matrix K determine the stability of the solution. It should be noted that due to the autonomous nature of the coupled-oscillator array one eigenvalue of K is always zero. The solution is stable if all remaining eigenvalues of K have negative real parts.

One can easily verify that K is unchanged to phase shifts that are common to all oscillators. This is due to the fact that matrix $D_\phi = D_\phi^R + j D_\phi^I$ contains only

phase differences between the various elements. It is then possible to reduce the system by one, thus eliminating the zero eigenvalue. Selecting an arbitrary element (for example, element j) as a reference, the N phase equations of Eq. (7.7-17) can be reduced by one by subtracting row $(N + j)$, the equation which corresponds to the phase of oscillator j , from every other equation. The equation that corresponds to the phase of oscillator j can then be eliminated. Furthermore, the elements of column $(N + j)$ from row $(N + 1)$ to $(2N)$ are multiplied by zero. In addition, in the amplitude equations, due to the fact that D_{ϕ}^R contains only phase differences, it is possible to subtract $\delta\phi_j$ from all phases forming $D_{\phi}^R \delta\phi \leftarrow D_{\phi}^R (\delta\phi - \delta\phi_j \mathbf{1})$. As a result column $(N + j)$ can also be eliminated because it is being multiplied by zero. The remaining square matrix $\tilde{\mathbf{K}}$ of dimension $N - 1$ has the same eigenvalues with \mathbf{K} minus the zero eigenvalue. Matrix $\tilde{\mathbf{K}}$ corresponds to the system of $2N - 1$ linear differential equations

$$\begin{bmatrix} \delta\dot{V} \\ \delta\dot{\tilde{\phi}} \end{bmatrix} = \tilde{\mathbf{K}} \begin{bmatrix} \delta V \\ \delta\tilde{\phi} \end{bmatrix} \quad (7.7-18)$$

where the vector $\delta\tilde{\phi}$ of dimension $N - 1$ contains phase difference terms relative to oscillator j . The spectral abscissa of a square matrix is the maximum real part of its eigenvalues [119]. Therefore a steady-state solution is stable if the spectral abscissa of $\tilde{\mathbf{K}}$ is negative.

7.8 A Comparison between the Two Perturbation Models for Coupled Oscillator Systems

The similarity of the two models is made obvious by comparing the two expressions corresponding to the generalized phase model Eq. (7.4-4) and Eq. (7.6-8). The first model is defined for a parallel RLC tank with a nonlinear voltage-dependent current source that exhibits a third-order nonlinearity similar to the one described in Section 7.5 and shown in Fig. 7-6. In this case, the admittance looking at the output node of the circuit is given by

$$Y(V, \omega) = (Y_N(V) + G_L) + \frac{1}{jL\omega} + jC\omega \quad (7.8-1)$$

where $Y_N(V)$ contains the nonlinear admittance of the current source at the fundamental frequency component. The total admittance contains a real nonlinear admittance term that is amplitude dependent, plus the load admittance, and an imaginary term which is frequency dependent. As a result, a real derivative versus the amplitude and an imaginary admittance derivative versus the frequency are obtained:

$$\frac{\partial Y}{\partial V} = \frac{\partial Y_N}{\partial V} \tag{7.8-2}$$

$$\frac{\partial Y}{\partial \omega} = j2C$$

Furthermore, if we consider that for a parallel resonant circuit the external quality factor is given by

$$Q = \frac{\omega_o C}{G_L} \tag{7.8-3}$$

it is straightforward to verify that the Eqs. (7.4-4) and (7.6-8) are identical.

In general, active devices in microwave frequencies exhibit nonlinear susceptance as well as admittance, in addition to a nonlinear admittance that is frequency dependent. In other words a more general expression for the admittance at an oscillator circuit node is

$$Y(V, \omega) = G_N(V, \omega) + jB_N(V, \omega) \tag{7.8-4}$$

As a result, it is possible to view the alternative model (7.6-4) using complex admittance derivatives as a generalized version of (7.4-1).

7.9 Externally Injection-Locked COAs

The coupled-oscillator array is an autonomous system that behaves like a single distributed oscillator. However, there are several applications that require the array to be injection-locked to an external signal. The reason can be to control the phase distribution among the array elements [1], to reduce the array phase noise [97], to fix the array frequency [120], or to introduce modulation to the array [121] [122].

An external injection signal introduces an additive forcing term in the time-domain expression of the perturbed oscillator equation. In Section 7.5, it was demonstrated that the topology of a parallel RLC tank with a nonlinear voltage-dependent current source and an external-injection current term leads to the forced van der Pol equation.

The coupled-oscillator system of differential equations is derived by applying Kirchhoff's current or voltage law at a selected circuit node or loop of each oscillator circuit in the array. Specifically, in the parallel-tank topology, the corresponding equations are obtained by applying Kirchhoff's current law at the output nodes of each oscillator. In addition, these nodes correspond to the nodes where the coupling network is connected to each oscillator. However,

this does not always have to be the case, and the coupling network maybe connected to a different oscillator node.

The external-injection signal typically may not be applied at the circuit node where the coupled oscillator system is derived. In this case it is necessary to derive analytically, or using a circuit simulator, a transfer function, which relates the applied injection signal to an induced current or voltage at the node or loop where the system equation is applied. Alternatively, it is possible to consider that the nonlinear-oscillator admittance is a function of the injection signal. It should be noted that in the general case there maybe more than one injection signal applied, and that the injection signal may be coupled to the coupled-oscillator array using different topologies, such as direct injection or radiation coupling, as shown in Fig.7-8 [123].

Following the formulation of Chang et al. [123] where the authors assume a parallel resonance model for the oscillator elements, and they consider the external injection signal in the form of an additional current source in parallel with the oscillator tank, one has

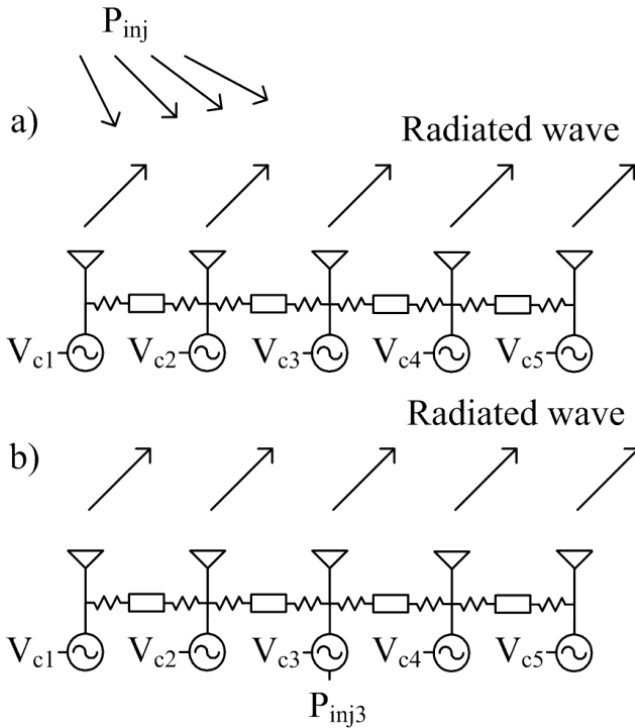


Fig. 7-8. Externally injection-locked coupled-oscillator array topologies, a) globally injected array, b) middle element injection.

$$\begin{aligned} \dot{A}_m = \mu(A_{om}^2 - A_m^2)A_m + \sum_{i=1}^N K_{mi}A_i \cos(\phi_i - \phi_m + \Phi_{mi}) \\ + K_{mp}A_p \cos(\phi_p - \phi_m + \Phi_{mp}) \end{aligned} \quad (7.9-1)$$

$$\begin{aligned} A_m \dot{\phi}_m = \Delta\omega_m A_m + \sum_{i=1}^N K_{mi}A_i \sin(\phi_i - \phi_m + \Phi_{mi}) \\ + K_{mp}A_{mp} \sin(\phi_{mp} - \phi_m + \Phi_{mp}) \end{aligned}$$

where it is assumed that oscillator m is being injected by an external source mp . The transfer function $\kappa_{mp} = t_{mp}\omega_m/2Q = K_{mp}e^{j\Phi_{mp}}$ consists of a complex normalized term t_{mp} multiplied with a scaling factor $\omega_m/2Q$ as is done for the coupling terms from the other oscillator elements in the array. For the case of an injection-current term in parallel with the oscillator tank $t_{mp} = 1$. Furthermore, when a single oscillator is considered, Eq. (7.9-1) reduces to Adler's equation.

Alternatively, it is possible to assume that the nonlinear oscillator admittance $Y_m(v_m, \omega, \mu, a_{mp})$ at the node under consideration additionally depends on the injection signal $a_{mp} = A_{mp}e^{j\phi_{mp}} = a_{mp}^R + ja_{mp}^I$ present at an arbitrary node of the oscillator circuit. Assuming a low amplitude-injection signal relative to the oscillator amplitude $\rho_{mp} = A_{mp}/A_m \ll 1$, a Taylor expansion of the oscillator admittance around the free running steady state gives, to first order, [124]

$$Y_m(v_m, \omega, \mu, a_{mp}) = Y_m(V_m, \omega, \mu) + Y_{mp}(\phi_m, a_{mp}) \quad (7.9-2)$$

with

$$\begin{aligned} Y_{mp}(\phi_m, a_{mp}) = \frac{\partial Y_{mp}}{\partial a_{mp}^R} A_{mp} \cos(\phi_{mp} - \phi_m) \\ + \frac{\partial Y_{mp}}{\partial a_{mp}^I} A_{mp} \sin(\phi_{mp} - \phi_m) \end{aligned} \quad (7.9-3)$$

The first term $Y_m(V_m, \omega, \mu)$ is the one considered in Eq. (7.6-3), where no external injection signal is present. The second term $Y_{mp}(\phi_m, a_{mp})$ is a linear perturbation term due to the external injection signal, which depends on the relative phase between the oscillator and the injection signal. The admittance expression is then introduced in the model presented in Section 7.6 and repeated here for convenience

$$Y_m V_m e^{j\phi_m} + \sum_{i=1}^N Y_{cmi} V_i e^{j\phi_i} = 0 \quad (7.9-4)$$

in order to derive the desired system of equations. As the injection power increases, additional terms in the Taylor expansion can be included in order to improve the accuracy of the approximation [124].

7.10 Phase Noise

Perturbation theory is applied in noise analysis of oscillators as typically noise is modeled as a stochastic forcing term in the oscillator differential equation. The stochastic nature of noise and the nonlinear nature of the oscillator circuits make noise analysis a challenging problem. Applying the averaging theory, Kurokawa [105] presented an elegant analysis of phase noise of free-running and externally injection locked oscillators. A fundamental assumption in his formulation is that noise, described by a time-domain stochastic process $n_m(t)$ can be expanded in a Fourier series around the arbitrarily chosen fundamental frequency ω_o as

$$n_m(t) = \sum_{n=-\infty}^{+\infty} N_{mn}(t) e^{j\omega_o t} \quad (7.10-1)$$

with $N_{mn}(t) = G_{mn}(t) + jB_{mn}(t)$ a complex noise process. In the following it is assumed that $n_m(t)$ is a zero-mean white Gaussian process, which results in $G_{mn}(t)$ and $B_{mn}(t)$ being uncorrelated white zero-mean Gaussian processes as well [105].

Extending the work of Kurokawa, Chang et al. [97] studied phase noise in mutually injection-locked coupled-oscillator arrays. Application of the noise expansion and averaging allows us to include the effect of noise in the oscillator formulation Eq. (7.4-1) in terms of $N_{m1}(t) = G_{m1}(t) + jB_{m1}(t)$. In the following, the subscript 1 is dropped for simplicity.

$$\begin{aligned} \dot{A}_m = & \mu(A_{om}^2 - A_m^2)A_m + \sum_{i=1}^N K_{mi}A_i \cos(\phi_i - \phi_m + \Phi_{mi}) \\ & - \frac{\omega_o}{2QG_L}G_m(t) \end{aligned} \quad (7.10-2)$$

$$\begin{aligned}
 A_m \dot{\phi}_m &= \Delta\omega_m A_m \\
 &+ \sum_{i=1}^N K_{mi} A_i \sin(\phi_i - \phi_m + \Phi_{mi}) \\
 &- \frac{\omega_o}{2QG_L} B_m(t)
 \end{aligned}$$

The solution of Eq.(7.10-2) is found in the form of a perturbation $(V_m + \delta V_m, \phi_m + \delta \phi_m)$ where (V_m, ϕ_m) is the solution to the noise-free system of Eq. (7.4-1), leading to a forced variational system, which is the same as was considered in the study of the stability of the steady state with the addition of a noise-forcing term. As before, small amplitude-noise perturbations δV_m and small phase-noise- perturbation differences $(\delta \phi_m - \delta \phi_i)$ result in the forced linear system of differential equations

$$\begin{aligned}
 \delta \dot{A}_m &= \mu(A_{om}^2 - 3A_m^2)\delta A_m \\
 &+ \sum_{i=1}^N K_{mi} \cos(\phi_i - \phi_m + \Phi_{mi}) \delta A_i \\
 &- \sum_{i=1}^N K_{mi} A_i \sin(\phi_i - \phi_m + \Phi_{mi}) (\delta \phi_i \\
 &- \delta \phi_m) - \frac{\omega_o}{2QG_L} G_m(t)
 \end{aligned} \tag{7.10-3}$$

$$\begin{aligned}
 A_m \delta \dot{\phi}_m &= (\Delta\omega_m - c)\delta A_m \\
 &+ \sum_{i=1}^N K_{mi} \sin(\phi_i - \phi_m + \Phi_{mi}) \delta A_i \\
 &+ \sum_{i=1}^N K_{mi} A_i \cos(\phi_i - \phi_m + \Phi_{mi}) (\delta \phi_i \\
 &- \delta \phi_m) - \frac{\omega_o}{2QG_L} B_m(t)
 \end{aligned}$$

Correspondingly, the alternative model in the presence of noise is modified by including an additive complex noise term $N_m(t) = G_m(t) + jB_m(t)$ in Eq. (7.6-4), which leads to forcing terms $G_m(t)$ and $B_m(t)$ in the left hand side of the first and second equations of Eq. (7.6-11), respectively. For compactness, the formulation is not repeated here.

Following Chang [97], we proceed to solve Eq. (7.10-3) by first applying a Fourier transform

$$\begin{aligned}
 j\Omega\delta\check{A}_m &= \mu(A_{om}^2 - 3A_m^2)\delta\check{A}_m \\
 &+ \sum_{i=1}^N K_{mi} \cos(\phi_i - \phi_m + \Phi_{im}) \delta\check{A}_i \\
 &- \sum_{i=1}^N K_{mi} A_i \sin(\phi_i - \phi_m + \Phi_{mi}) (\delta\check{\phi}_i \\
 &- \delta\check{\phi}_m) - \frac{\omega_o}{2QG_L} \check{G}_m
 \end{aligned} \quad (7.10-4)$$

$$\begin{aligned}
 j\Omega A_m \delta\check{\phi}_m &= (\Delta\omega_m - c)\delta\check{A}_m \\
 &+ \sum_{i=1}^N K_{mi} \sin(\phi_i - \phi_m + \Phi_{mi}) \delta\check{A}_i \\
 &+ \sum_{i=1}^N K_{mi} A_i \cos(\phi_i - \phi_m + \Phi_{mi}) (\delta\check{\phi}_i \\
 &- \delta\check{\phi}_m) - \frac{\omega_o}{2QG_L} \check{B}_m
 \end{aligned}$$

The frequency Ω indicates offset from the fundamental ω_o , and the hat indicates a Fourier transformed variable. The linear system of Eq. (7.10-4) is processed easier in matrix form. Using the formulation of Section 7.7, it is possible to write Eq. (7.10-4) in the form

$$\{j\Omega\mathbf{I} - \mathbf{D}\} \begin{bmatrix} \delta\check{\mathbf{A}} \\ \delta\check{\boldsymbol{\phi}} \end{bmatrix} = \mathbf{N} \begin{bmatrix} \delta\check{\mathbf{A}} \\ \delta\check{\boldsymbol{\phi}} \end{bmatrix} = \begin{bmatrix} \check{\mathbf{G}}_n \\ \check{\mathbf{B}}_n \end{bmatrix} \quad (7.10-5)$$

or

$$\begin{bmatrix} \delta\check{\mathbf{A}} \\ \delta\check{\boldsymbol{\phi}} \end{bmatrix} = \mathbf{P} \begin{bmatrix} \check{\mathbf{G}}_n \\ \check{\mathbf{B}}_n \end{bmatrix} \quad (7.10-6)$$

with $\mathbf{P} = \mathbf{N}^{-1} = [j\Omega\mathbf{I} - \mathbf{D}]^{-1}$ where the noise terms have been normalized as $\check{\mathbf{G}}_n = -\frac{\omega_o}{2QG_L} [\check{G}_m]$ and $\check{\mathbf{B}}_n = -\frac{\omega_o}{2QG_L} [\check{B}_m]$ for compactness. It should be clarified that the identity matrix in Eq. (7.10-5) is of dimension $2N$. Correspondingly, the formulation pertaining to the generalized phase model is

$$\{j\Omega\mathbf{I} - \mathbf{D}_G\} \delta\check{\boldsymbol{\phi}} = \mathbf{N}_G \delta\check{\boldsymbol{\phi}} = \check{\mathbf{B}}_n \quad (7.10-7)$$

or

$$\delta\check{\phi} = P_G \check{B}_n \tag{7.10-8}$$

with $P_G = N_G^{-1} = [j\Omega I - D_G]^{-1}$.

The noise correlation matrix $S(\Omega)$ of the oscillator array is given by

$$S(\Omega) = \langle [\begin{smallmatrix} \delta\check{A} \\ \delta\check{\phi} \end{smallmatrix}] [\delta\check{A}^H \quad \delta\check{\phi}^H] \rangle = \begin{bmatrix} S_{AA} & S_{A\phi} \\ S_{\phi A} & S_{\phi\phi} \end{bmatrix} \tag{7.10-9}$$

where the superscript $()^H$ denotes the conjugate transpose operation. The various noise contributions AM-AM AM-PM, PM-AM, and PM-PM are easily identified.¹ The operator $\langle \ \rangle$ denotes ensemble average, and following [97], for white Gaussian processes one has

$$\langle \check{G}_n \check{G}_n^H \rangle = \langle \check{B}_n \check{B}_n^H \rangle = \left(\frac{\omega_o \sigma}{2QG_L} \right)^2 I \tag{7.10-10}$$

$$\langle \check{G}_n \check{B}_n^H \rangle = \langle \check{B}_n \check{G}_n^H \rangle = \mathbf{0}$$

with σ^2 as the noise variance. Identical oscillators have been assumed and identical noise sources have been applied at each oscillator for simplicity. The spectral density of the oscillator array is given by the diagonal of $S(\Omega)$.

The noise correlation matrix is then given by

$$S(\Omega) = \left(\frac{\omega_o \sigma}{2QG_L} \right)^2 P P^H \tag{7.10-11}$$

The generalized phase model expression can be used to obtain an approximate, more simplified, expression for the correlation matrix $S_G(\Omega)$, without considering amplitude noise:

$$S_G(\Omega) = \left(\frac{\omega_o \sigma}{2QG_L} \right)^2 P_G P_G^H \tag{7.10-12}$$

Note that $S_G(\Omega)$ is a square matrix of dimension N containing all correlation terms among the noise quantities of the individual oscillators. The phase noise spectra $S_{G\phi}(\Omega)$ of the individual oscillators in the array are given by the diagonal elements of $S_G(\Omega)$, or

$$S_{G\phi}(\Omega) = \left(\frac{\omega_o \sigma}{2QG_L} \right)^2 \text{dg}\{P_G P_G^H\} \mathbf{1} \tag{7.10-13}$$

¹ AM is amplitude modulation, and PM is phase modulation.

The phase noise spectrum $S_{1\phi}(\Omega)$ of a single oscillator element uncoupled to the rest of the array corresponds to $\mathbf{D}_G = \mathbf{0}$, and is given by

$$S_{1\phi}(\Omega) = \left(\frac{\omega_o \sigma}{2Q G_L} \right)^2 \frac{1}{\Omega^2} \quad (7.10-14)$$

This expression is in agreement with the one given by Kurokawa in Ref. [105] and demonstrates the dependence of Ω^{-2} of the phase-noise spectrum for the case of white Gaussian noise sources.

The expression for the phase noise spectrum vector $\mathbf{S}_{G\phi}(\Omega)$ of each oscillator element in the array finally can be written

$$\mathbf{S}_{G\phi}(\Omega) = S_1(\Omega) \Omega^2 \text{dg}\{\mathbf{P}_G \mathbf{P}_G^H\} \mathbf{1} \quad (7.10-15)$$

In addition to the phase noise of the individual coupled oscillator elements $\delta\phi_m$, in quasi optical power combining applications, one is also interested in the phase noise of the combined output of the oscillators $\delta\phi_T$. Assuming small perturbations, one may write the combined far-field amplitude $V(t)$ as [97]

$$\begin{aligned} V(t) &= \sum_{m=1}^N A_m \cos(\omega_o t + \phi_m) \\ &\approx NA \sum_{m=1}^N \cos(\omega_o t + \phi_T) \end{aligned} \quad (7.10-16)$$

with

$$\delta\phi_T = \frac{1}{N} \sum_{m=1}^N \delta\phi_m = \frac{1}{N} \mathbf{1}^T \delta\phi \quad (7.10-17)$$

The phase noise spectrum $S_{GT}(\Omega)$ of the combined output is given by

$$S_{GT}(\Omega) = \langle \delta\check{\phi}_T \delta\check{\phi}_T^H \rangle = \frac{1}{N^2} \langle \mathbf{1}^T \delta\check{\phi} \delta\check{\phi}^H \mathbf{1} \rangle \quad (7.10-18)$$

which, with the help of Eq. (7.10-15) becomes

$$S_{GT}(\Omega) = \frac{S_1(\Omega) \Omega^2}{N^2} \mathbf{1}^T \mathbf{P}_G \mathbf{P}_G^H \mathbf{1} \quad (7.10-19)$$

Evaluation of the individual oscillator phase noise and the combined output phase noise is generally possible only by numerically evaluating Eqs. (7.10-15) and (7.10-19) respectively. Nonetheless, Chang et. al. [97] were able to analytically study several cases commonly found in the literature.

One of the results obtained by Chang, et al. [97] corresponds to the case where $\mathbf{D}_G = [\Phi^H \kappa \Phi - \text{dg}(\Phi^H \kappa \Phi \mathbf{1})]^R$, repeated here for convenience, is a symmetric matrix ($\mathbf{D}_G^T = \mathbf{D}_G$). As one can see, \mathbf{D}_G depends both on the coupling network through κ , and on the steady-state phase distribution of the various oscillator array elements, through Φ . It can be easily verified that $\mathbf{D}_G \mathbf{1} = \mathbf{0}$, which reflects the fact that the steady state is unchanged to within a common constant phase term added to all oscillator elements, or in other words, the fact that the steady state is defined by the phase differences of the various elements. Using the above two properties, Chang et al. [97] have shown by analytically evaluating $\mathbf{P}_G \mathbf{P}_G^H$ that $\mathbf{1}^T \mathbf{P}_G \mathbf{P}_G^H \mathbf{1} = \Omega^{-2} N$, which results in

$$S_{GT}(\Omega) = \frac{S_1(\Omega)}{N} \tag{7.10-20}$$

This is an important result indicating that the phase noise of the combined array output is reduced by a factor N compared to the individual free-running oscillator phase noise (as indicated in Section 6.4). It remains to identify under which conditions \mathbf{D}_G is symmetric. One characteristic example is when an in-phase steady-state solution is assumed ($\Phi = \mathbf{I}$) and a reciprocal coupling network matrix with zero coupling phase $\kappa^T = \kappa = \kappa^R$.

In the case of a reciprocal coupling network of near-neighbor bilateral coupling with zero coupling phase, \mathbf{D}_G is symmetric for any constant phase distribution among the oscillator elements. It was also shown that in this case the individual oscillator phase noise is also reduced by a factor N when the oscillators are in-phase. The oscillator phase noise for steady states with phase distributions with non-zero progressive phase $\Delta\phi_p$ degrades with increasing $\Delta\phi_p$ up to the point where the array loses stability and the phase noise becomes equal to the free-running oscillator phase-noise value.

Finally, it was shown by Chang et al. [97] that there is no phase noise improvement in the case of unilaterally coupled oscillators, both for the individual elements and the combined-array output (as indicated in Section 6.4).

The phase noise of externally injection-locked oscillators has been investigated by Kurokawa in [105], where it was shown that the injected oscillator phase-noise spectrum follows the phase-noise profile of the injection-locking signal for small frequency offsets near the carrier, and it converges to the free-running oscillator phase-noise spectrum for large frequency offsets. The formulation of Kurokawa [105] was extended to externally injection locked coupled oscillator arrays by Chang, et al. [123]. It is straightforward to obtain the formulation pertaining to the externally injection-locked coupled-oscillator arrays by

properly including in Eq. (7.10-2) terms due to injection sources as shown in (7.9-1). Chang et al. [123] investigated several topologies including a globally injected linear array, and arrays where a different single elements within the array are injected. In summary, the results showed that for small offsets the array phase-noise profile follows the injection-locking source phase-noise profile. However, for large offsets from the carrier the globally illuminated case showed a different behavior than the single-element illumination topology. In the former, the phase noise improves with increasing number of array elements, whereas in the latter the phase noise degrades with increasing number of elements. Furthermore, the array phase-noise performance of the single-element injection case improves as one injects an element closer to the array center.

7.11 Modulation

Several authors have considered the use of coupled-oscillator arrays in communication system applications. It is possible to distinguish among architectures where the coupled-oscillator array signal is modulated or architectures employing a coupled-oscillator array as the local oscillator in a multi-antenna up-converting or down-converting transceiver. The first topology has been studied by Kykkotis et. al. in [99]. Due to the limiting properties of oscillators, modulation formats that lead to large variations in the signal envelope are not recommended as the oscillator dynamics will tend to smooth these variations and introduce distortion. However, constant envelope modulation formats (such as constant phase modulation (CPM) and Gaussian minimum shift keying (GMSK)) represent excellent candidates to be employed in such systems. In Ref. [99], the modulation is applied in the coupled-oscillator array through an external injection signal. Additionally, it is possible to introduce modulation through the frequency-tuning bias voltage of the individual oscillators, as was proposed by Pogorzelski in Ref. [63].

A formulation based on Eq. (7.9-3) where the effect of the external-injection signal is included in the oscillator admittance was used by Collado and Georgiadis [124] to analyze the performance of such systems as the modulation bandwidth increases. The effect of the modulation on the maximum stable progressive constant phase shift among the oscillator elements was investigated, and it was shown that the presence of modulation leads to a reduction of the maximum achievable scanning range. In Fig. 7-9, the effect of sinusoidal phase modulation in the maximum scanning range of a two-element coupled oscillator array is shown. The maximum stable phase difference between the first harmonics of the two oscillators is obtained using the aforementioned model (denoted by RoM in Fig. 7-9), in good agreement with measurements as well as simulation results obtained using a commercial envelope transient circuit simulator. (The principles of nonlinear-circuit

simulation methods, such the envelope transient, are described in Chapter 8.) In addition, measurements of the maximum phase difference of the second harmonics of the oscillators are presented, and compared with the results using the envelope transient simulator. As can be seen from Fig. 7-9, extended scanning range can be obtained by considering the phase variation of an oscillator harmonic frequency rather than the fundamental frequency. Such architectures used to provide extended phase-scanning range are described in Section 8.6.

On the other hand, the use of coupled-oscillator arrays to provide the local oscillator signal in multi-element communication transceivers has been studied by Pogorzelski and Chiha in Ref. [74] and Pogorzelski in Ref. [125]. The coupled-oscillator array is used to provide a local-oscillator signal to a mixer with a desired phase distribution in order to appropriately steer the array beam without the need for phase shifters and a complex local-oscillator distributed feed network. In addition, more compact front ends can be implemented employing an array of coupled self-oscillating mixers as was proposed by ver Hoeye et al. [79].

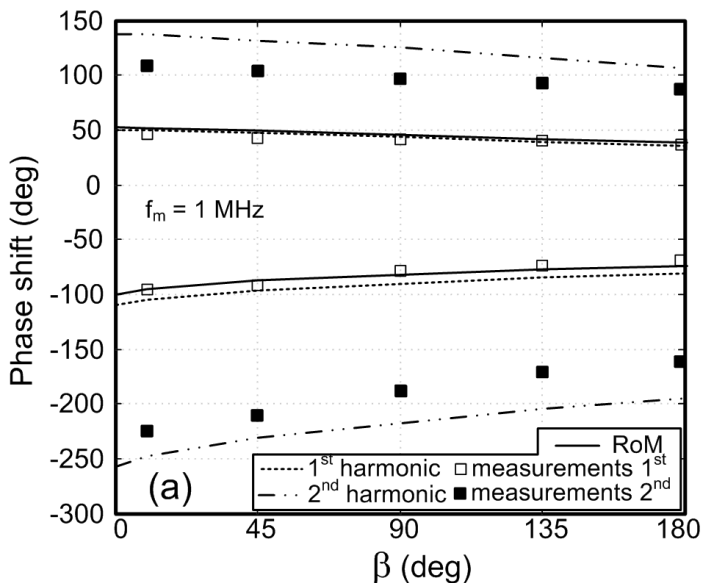


Fig. 7-9. Two-element coupled-oscillator array. Effect of phase modulation index β on stable phase shift among the oscillator elements. Sinusoidal phase modulation of 1 MHz frequency is applied by external injection locking to the one oscillator of the array. The results of the model developed based on Eq. (7.9-3) are denoted by RoM. (Reprinted with permission from [124], ©2001 IEEE.)

7.12 Coupled Phase-Locked Loops

A phase-locked loop (PLL) is typically used in frequency-generation applications, as well as in phase recovery and phase/frequency modulation/demodulation applications where one oscillator is required to track the phase of a signal present at its input. Therefore, it presents an excellent candidate for generating phase distributions among oscillator elements, which are required in electronic beam-steering applications. Martinez and Compton [126] first proposed the use of a coupled phase-locked loop for phased arrays. Subsequently, Buckwalter et. al. [127] extended their work to study the synchronization properties of such loops, and Chang presented a phase noise analysis [128].

The topology of a coupled PLL system is shown in Fig. 7-10, where a linear array of oscillators is considered. An error signal e is formed by a mixing operation where the outputs of adjacent oscillators are multiplied together. The mixers are used as phase detectors; however, other more sophisticated topologies can also be used where the oscillator outputs are first passed through a frequency divider and are subsequently fed to a digital phase detector, as is typically done in PLL architectures. Finally, the loop is closed by feeding the error signal to each oscillator-control input after it has passed through a loop filter. The relative phases between the oscillator elements are controlled by introducing additional external signals in the error signal path such as x_1 and x_N , shown in Fig. 7-10.

In the following, an introduction to the equations describing the dynamics of a two-element coupled PLL system is presented, following the formulation by Buckwalter et al. [127], and based on the topology indicated in Fig. 7-10. Identical oscillators are assumed where, for simplicity, a linear voltage-to-frequency model relation is considered

$$\dot{\phi}_i = \omega_i + K_v y_i \quad (7.12-1)$$

The index $i = 1, 2$ runs through the set of two oscillators. Furthermore, a first-order loop filter is assumed with gain a , one zero τ_z , and one pole τ_p , having a transfer function given by

$$H(\omega) = a \frac{1 + j\omega\tau_z}{1 + j\omega\tau_p} \quad (7.12-2)$$

Identical loop filters are considered for both oscillators.

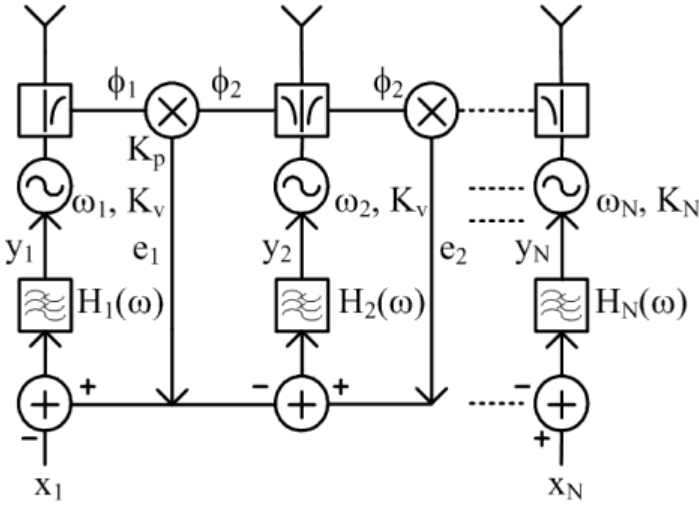


Fig. 7-10. Coupled phase-locked loop architecture.

Based on Fig. 7-10, and considering two oscillators the following system of equations is derived

$$\tau_p \dot{y}_1 + y_1 = a[\tau_z(\dot{e}_1 - \dot{x}_1) + (e_1 - x_1)] \tag{7.12-3}$$

$$\tau_p \dot{y}_2 + y_2 = a[\tau_z(\dot{x}_2 - \dot{e}_1) + (x_2 - e_1)] \tag{7.12-4}$$

$$\dot{\phi}_1 = \omega_1 + K_v y_1 \tag{7.12-5}$$

$$\dot{\phi}_2 = \omega_2 + K_v y_2 \tag{7.12-6}$$

$$e_1 = K_p \sin \phi_1 \sin \phi_2 \approx \frac{1}{2} K_p \cos(\phi_2 - \phi_1) \tag{7.12-7}$$

It should be noted that for the sake of simplicity the higher frequency mixing product is not considered in the error signal e_1 as it is assumed that it will be greatly attenuated by the loop filter.

Using the above equations, it is possible to derive one equation governing the dynamics of the phase difference $\Delta\phi = \phi_2 - \phi_1$. The external signals x_1 and x_2 can be used to introduce modulation to the loop or simply set some desired phase difference by introducing some offset to the equilibrium point of the loop. Setting external signals equal to zero ($x_1 = x_2 = 0$) it is straightforward to derive the differential equation that the phase difference between the oscillators satisfies

$$\tau_p \Delta \ddot{\phi} + [1 - \tau_z G \sin \Delta \phi] \Delta \dot{\phi} + G \cos \Delta \phi - \Delta \omega = 0 \quad (7.12-8)$$

where $\Delta \omega = \omega_2 - \omega_1$ and $G = \alpha K_v K_p$. The equilibrium points of the coupled PLL correspond to $\Delta \ddot{\phi} = \Delta \dot{\phi} = 0$ and are derived by solving

$$G \cos \Delta \phi - \Delta \omega = 0 \quad (7.12-9)$$

It is easy to verify that two solutions exist within the phase interval $[0, 2\pi)$, and perturbation analysis of Eq. (7.12-8) can be used to show that only the one of the two that falls in the interval $[0, \pi)$ is stable [127]. This fact implies that the phase difference of the two oscillators for the topology under consideration can be tuned in the range $[0, \pi)$, by varying the relative frequencies of the two oscillators $\Delta \omega$.

The hold-in range Ω_h of the coupled PLL is the range of the frequency difference among the oscillator elements for which the system remains in a stable equilibrium. The pull-in range on the other hand, is the range of the frequency difference for which the system will eventually evolve to a stable equilibrium. The hold-in range presents an upper bound to the pull-in range. Based on the above analysis and the stability analysis of the equilibrium points, it was determined by Buckwalter, et al. [127] that the hold-in range is equal to

$$\Omega_h = 2G \quad (7.12-10)$$

Furthermore, they calculated an approximate value for the pull-in range as given by Eq. 7.12-11 [127]

$$\Omega_p \approx 2 \sqrt{\frac{\sqrt{1 + 4\tau_p^2 G^2} - 1}{2\tau_p^2}} \quad (7.12-11)$$

Finally, Buckwalter, et al. [127] studied the effect of circuit delay on the hold-in and pull-in range of the system. Such delays are present in the system due to the filter characteristics of the circuit, and they result in complex dynamic behavior and instabilities. We remark that such filter characteristics may be fruitfully interpreted as time delays if the delay is small. Unlike Chapter 5 of this book, the analysis of Buckwalter, et al. does include the nonlinear behavior. Recall that in Chapter 5 we introduced coupling delay in oscillator arrays via an exponential of the Laplace transform variable. There the analysis was done in the linear approximation, and thus the solutions did not exhibit any of the complex dynamical behavior arising from nonlinearity. The delay introduced was a true time delay due to propagation through the coupling lines and was not constrained to be small. However, the late time behavior in that situation

corresponds to solution at time equal to many delay times, a condition which may be satisfied either by large t or small delay or both.

The model described in this section can be made progressively more complex, by taking into account the high-frequency mixing product at the output of the phase detector in the formulation, or by using a higher order loop filter and digital phase detectors.

7.13 Conclusion

In this chapter we revisited the analysis of coupled-oscillator arrays and presented two approximate models that describe the amplitude and phase dynamics at the fundamental frequency of oscillation of the coupled oscillator arrays. We presented a compact matrix formulation of the models, which can be used to efficiently analyze the transient behavior of the arrays, determine the various steady-state solutions, and examine their stability. In addition we provided a formulation that enables one to consider external injection-locking signals to the array, which can be used to introduce modulation into the array. These models were used to provide an overview of the phase-noise analysis of coupled-oscillator arrays. Such approximate models can be used to simulate large coupled-oscillator arrays in a computationally efficient manner. Finally, it was pointed out that PLLs can be substituted for VCOs in coupled systems, resulting in behavior quite similar to that of the arrays discussed previously. In the next chapter we describe nonlinear simulation methods that can be used to accurately simulate and design oscillator circuits and coupled-oscillator arrays.

